Tracking Performance at CMS

D. Giordano,
on behalf of the CMS Collaboration
CERN, European Organization for Nuclear Research,
Geneva, Switzerland

The first LHC collisions at center of mass energies of 900 GeV and 2360 GeV were recorded by the CMS detector in December 2009. The trajectories of charged particles produced in the collisions were reconstructed using the all-silicon CMS Tracker and their momenta were measured in the 3.8 T solenoidal magnetic field. In this paper the results from track reconstruction are presented to demonstrate the overall performance of the CMS Tracker.

1 Introduction

CMS [1] is one of the four detectors at the Large Hadron Collider (LHC) of CERN. It has been designed primarily to perform new physics studies at the highest energies achievable with the LHC. The main components of CMS are a muon detection system, electromagnetic and hadronic calorimeters, and an inner tracking system (Tracker). The Tracker provides robust, efficient, and precise reconstruction of the charged particle trajectories inside a 3.8 T axial magnetic field. The design transverse momentum resolution is typically 0.7 (5)% at 1 (1000) GeV/c in the central region and the impact parameter resolution for high momentum tracks approaches 10 μm.

The CMS Tracker [1], consists of two main detectors: a Silicon Pixel Detector, located close to the interaction region, and a Silicon Strip Detector, covering the region from $\approx$ 25 cm to $\approx$110 cm in radius, and $\approx$ 270 cm on either side of the collision point along the LHC beam axis. The pixel detector has 66 million active elements instrumenting a surface area of about 1 m^2. It is designed to provide three high precision three-dimensional determinations of particle trajectory points. The strip detector has 9.3 million active elements instrumenting a surface area of 198 m^2. It is designed to provide 9-13 high precision determinations of particle trajectory points in the region of pseudorapidity $|\eta| < 2.4$; about half of the coordinates originate from a sensor pair where one of the two sensors is tilted by 0.1 radians, hence providing also a measurement of the z coordinate.

The results presented in this paper were obtained using data samples collected by the CMS experiment during LHC operation in December 2009 at proton-proton center-of-mass energies of 900 GeV and 2360 GeV. Due to the relatively low LHC luminosity, the event selection was mainly based on a minimum bias trigger system consisting of beam scintillator counters [2]. The total number of selected minimum bias events is about 305 000, corresponding to an integrated luminosity of approximately 10 μb^{-1} at 900 GeV and 0.4 μb^{-1} at 2360 GeV.

Prior to the LHC *pp* collisions, the CMS detector was commissioned using about 10 million cosmic muon events, collected under detector and magnetic field conditions similar to the conditions during *pp* collisions [3]. The analysis of cosmic muon data provided good initial operating

points for the pixel detector, the strip detector and the tracker alignment. For instance, the precision achieved for the Tracker alignment parameters (∼3-4 μm in the pixel barrel local x and y coordinates) is already adequate for the precise determination of impact parameters and the reconstruction of secondary vertices.

2 Track Reconstruction

The track reconstruction algorithms rely on a good estimate of the proton-proton interaction region, referred to as the beamspot. The beamspot is used as a precise estimate of the primary interaction point (in the transverse direction) prior to primary vertex reconstruction. After the beamspot is known, an initial round of tracking and vertexing is done using only pixel hits. The pixel vertices found at this stage are used in the standard tracking.

The standard track reconstruction at CMS is performed by the combinatorial track finder (CTF) [4]. Tracks are seeded from either triplets of hits in the tracker or pairs of hits with an additional constraint from the beamspot or a pixel vertex, yielding an initial estimate of the trajectory, including its uncertainty. The seed is then propagated outward in a search for compatible hits. As hits are found, they are added to the trajectory and the track parameters and uncertainties are updated. This search continues until either the boundary of the tracker is reached or no more compatible hits can be found. An additional search for hits is performed starting from the outermost hits and propogating inward. In the final step, the collection of hits is fit to obtain the best estimate of the track parameters, and tracks are filtered to remove those that are likely fakes.

The current implementation of the CTF performs multiple iterations. Between each iteration, hits that can be unambiguously assigned to tracks in the previous iteration are removed from the collection of tracker hits to create a smaller collection that can be used in the subsequent iteration. The first iterations look for prompt tracks, progressively of lower momentum. The following iterations are intended to find displaced tracks or tracks lacking pixel hits.

Finally, starting from the track collection, the primary interaction vertices in the event are reconstructed using an adaptive vertex fit.

3 Tracking Performance

Before using the tracks in further reconstruction of resonances or other objects, a comparison of basic distributions (number of hits per track, transverse momentum, angular parameters impact parameters, normalized χ^2) between the data and simulation was performed, revealing a general agreement in the shape of all variables.

After that, a careful study of the primary vertex and the beamspot reconstruction was performed. The beamspot measurement was performed during each LHC fill, confirming the stability of the luminous region along these first runs: variations in the position of the beamspot were at the level of ∼0.5 mm in x and y and ∼2 cm in z.

The resolution of the primary vertex was evaluated as a function of the two quantities that most affect this measurement: the multiplicity of tracks used in fitting the vertex and the p_t of those tracks. Figure 1 shows the x and z resolutions for different average p_t ranges. While the resolution differs considerably depending on p_t and multiplicity, the simulation accurately reproduces the data results.

More details about the tracking performance during the 2009 data-taking can be found at [5].

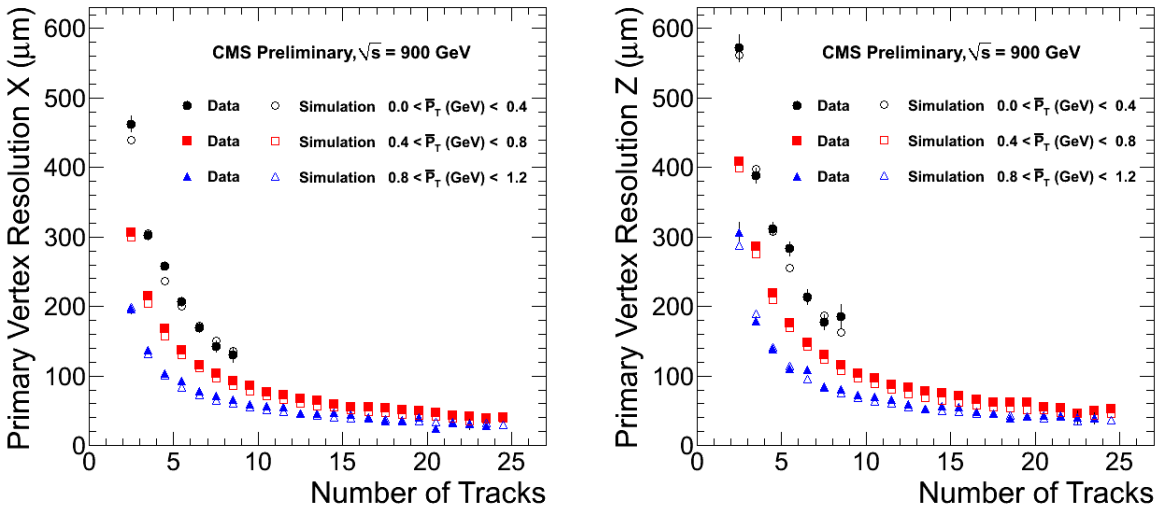

(a) (b)

Figure 1: Primary vertex resolution in x (a) and z (b) versus number of tracks. The three sets of results in each plot show different average p_t ranges and within each p_t range, data and simulation are compared.

3.1 Reconstruction of Resonances

The collection of tracks was then used to reconstruct the decays of K^0_S, Λ^0, $\Xi^{\pm}$, and $K^{\star}(892)$. The measurement of the masses and lifetimes of these well-known particles provides an initial validation of the reconstruction (for both prompt and displaced tracks), vertexing, and the magnetic field.

The K^0_S and Λ^0 candidates were reconstructed by their decay to $\pi^+\pi^-$ and $p\pi^-$ (+ charge conjugate), respectively. The K^0_S candidates were then combined with charged tracks from the primary vertex to search for the strong decay $K^*(892)^- \to K^0_S\pi^-$. The Ξ^- was reconstructed through its decay to $\Lambda^0\pi^-$. As the Ξ^- is a long-lived baryon, the π^- from the Ξ^- decay is detached from the primary vertex rather than originating from the primary vertex.

The mass distributions, along with the overlaid fits, are shown in Fig. 2. The mass values obtained fitting the data distributions are in good agreement with the world average values (PDG [6]), as shown in Table 1.

Table 1: Summary of PDG and data masses. Uncertainties for data results are statistical only.

	Mass (MeV/c^2)	
particle	Data	PDG
K^0_S	497.68 ± 0.06	497.61 ± 0.02
Λ^0	1115.97 ± 0.06	1115.683 ± 0.006
$K^*(892)^{\pm}$	888.3 ± 3.2	$891.66 \pm .26$
Ξ^-	1322.8 ± 0.8	1321.71 ± 0.07

For the K^0_S and Λ^0, the lifetime was also measured. The yield of the reconstructed candidates under the mass peak was correlated with the proper decay length ($ct = mL/p$) of the candidates. Appropriate correction factors, evaluated on simulated data, were applied to the measured yield, in order to take into account the efficiency variation versus lifetime. The goodness of the exponential fit of the calibrated yield versus ct indicates the accuracy of the estimated correction factors. The results, $\tau_{K^0_S} = 90.0 \pm 2.1$ ps and $\tau_{\Lambda^0} = 271 \pm 20$ ps, are both within 1 σ of the world average [6].

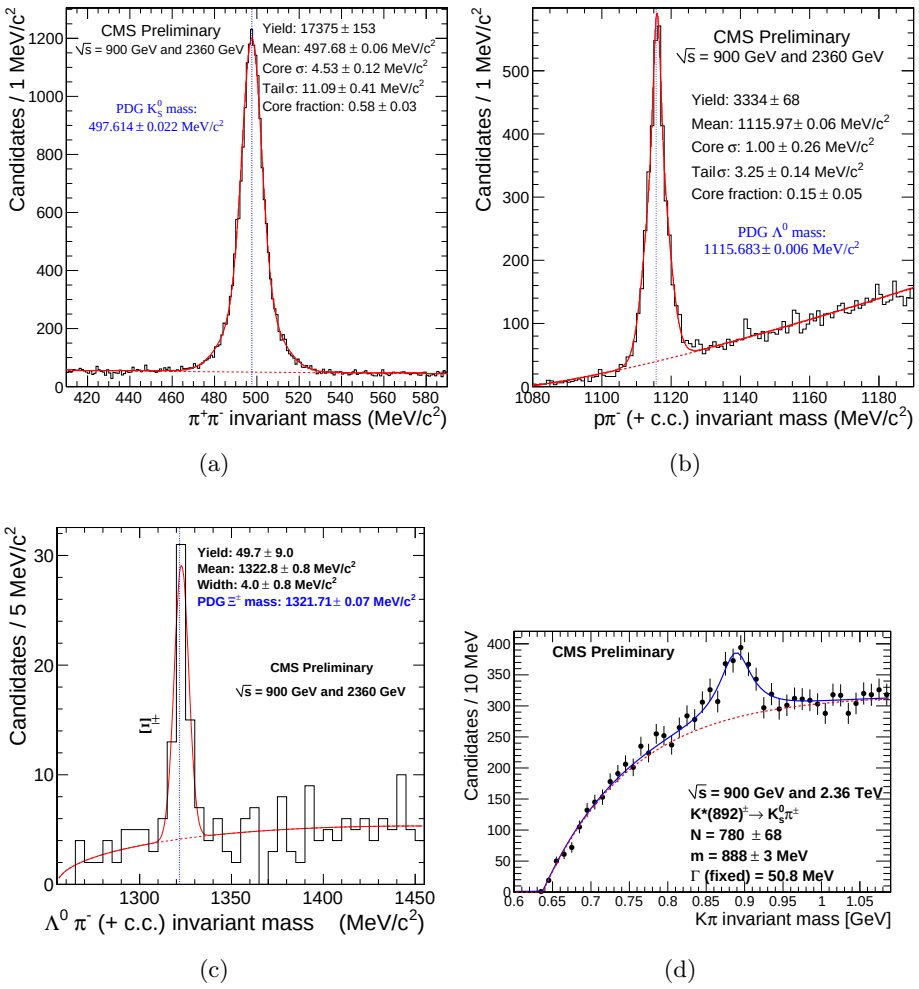

Figure 2: Invariant mass, with fit, of the $\pi^+\pi^-$ pairs - for the K^0_S - (a), of the $p\pi^-$ (+ charge conjugate) pairs - for the Λ^0 - (b), of the $\Lambda^0\pi^-$ (+ charge conjugate) pairs - for the $\Xi^\pm$ - (c), and of the $K^0_S\pi^-$ (+ c.c.) pairs - for the $K^*(892)^\pm$. Uncertainties shown are statistical only.

3.2 Particle identification with dE/dx

Although the primary function of the strip tracker is to provide hit position information for track reconstruction, the charge collected in a hit cluster provides a measure of the energy loss (dE/dx) of a particle while traversing the silicon sensor. A dE/dx estimator based on the measurements in the strip tracker modules traversed by a particle, is used in combination with the measured momentum p of the track to identify the mass (particle type) of the traversing particle.

Figure 3(a) shows the relationship between the dE/dx estimator and momentum in the 900 GeV data. In the figure, clear bands can be seen for kaons and protons and to a much lesser extent for deuterons. Figure 3(b) shows the mass distribution of tracks as determined by the same dE/dx methods. Clear kaon and proton peaks can be observed, as well as good agreement for the peaks with a Monte Carlo simulation. The particle identification technique was validated for protons and kaons using data driven methods based on reconstructed samples of $\Lambda^0 \to p\pi^-$ and $\phi(1020) \to K^+K^-$ decays. These decays provide clean samples of protons and kaons, subsequently identified by the dE/dx tool. This technique can be used to aid in the detection of very massive charged states, such as heavy stable charged particles [7].

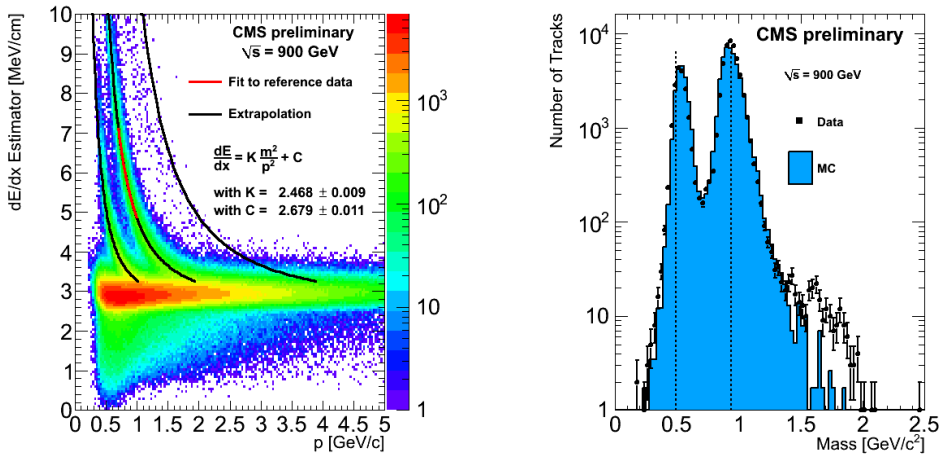

(a) (b)

Figure 3: dE/dx estimator versus particle momentum (a). Frequency of tracks as a function of mass as determined by the measured energy loss (b). The generator used for the simulation, PYTHIA, does not produce deuterons, although they can be produced in the subsequent GEANT hadron showers. This explains the observed deficit in the Monte Carlo prediction.

3.3 Reconstruction of Photon Conversions and Nuclear Interactions

Photon interactions with the tracker material can produce e^+e^- conversion pairs while for hadrons, a nuclear interaction can produce multiple hadrons. These interactions could reduce the efficiency for low energy photon finding by the electromagnetic calorimeter, as well as the resolution of many hadronic observables such as jets or missing transverse energy. To improve the description of the reconstructed event the identification of conversions and nuclear interactions is part of the tracker reconstruction.

The December 2009 collision data allowed to validate the performance of the identification procedures, and to confirm our understanding of the material in the Tracker. For instance, the distribution of the interaction positions provides a means of observing material in the detector. The distribution versus radial position ρ of the nuclear vertices, compared to the simulation, is shown in Fig. 4. The simulation histogram is normalized to the total number of nuclear interactions found in data in the full z range. The good agreement between the data and simulation indicates a consistent description of the material distribution in this region.

4 Conclusions

The performance of the CMS Tracker has been studied using the collision data at center-of-mass energies of 0.9 and 2.36 TeV. The tracking and vertexing resolutions are in agreement with the expected design performance in minimum bias events, for the level of the alignment achieved. Studies of the decays of K^0_S, Λ^0, Ξ^-, and $K^*(892)^-$ test the capability to reconstruct displaced vertices and agree well with predictions from simulation, providing strong tests of our understanding of the magnetic field, tracker material, and detector performance. The accuracy of the tracker material description is demonstrated by the agreement between data and simulation for photon conversions and nuclear interactions. Ionization energy loss measurements in the tracker provide good particle identification at low momentum.

The excellent tracking performance in the early collision running demonstrates that the all-silicon CMS Tracker fully meets its design specifications.

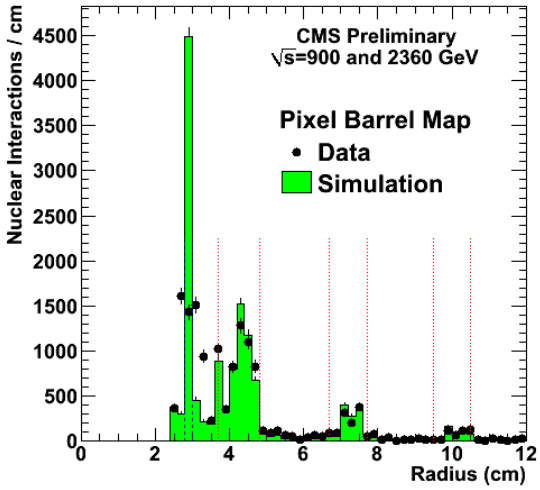

Figure 4: The nuclear interaction vertices: distribution of the radial position ρ for $|z| < 26$ cm. The beam pipe at radius of 3 cm, as well as the three barrel pixel layers at average radii of 4.3 cm, 7.3 cm, and 10.2 cm, are clearly seen. In the data, the beam pipe center is offset from the pixel detector center resulting in a smeared distribution versus radius.

References

1. CMS Collaboration. The CMS experiment at the CERN LHC. *JINST* **0803**, S08004 (2008).
2. CMS Collaboration. Transverse momentum and pseudorapidity distributions of charged hadrons in pp collisions at $\sqrt{s} = 0.9$ and 2.36 TeV. *JHEP* **02**, 04 (2010).
3. CMS Collaboration. Commissioning of the CMS experiment and the cosmic run at four tesla. *JINST* **5**, T03001 (2010).
4. W. Adam, B. Mangano, Th. Speer, and T. Todorov. Track Reconstruction in the CMS Tracker. *CMS Note* **2006/041**, (2006).
5. CMS Collaboration Tracking and Vertexing Results from First Collisions. http://cms-physics.web.cern.ch/cms-physics/public/TRK-10-001-pas.pdf *CMS Physics Analysis Summary* **TRK-10-001**, (2010)
6. C. Amsler et al. Review of Particle Physics. *Physics Letters* **B667**, 1 (2008).
7. M. Fairbairn et al. Stable massive particles at colliders. *Phys. Rept.* **438**, 1–63 (2007).